

Efficient stabilizer entropies for quantum computers

Tobias Haug,^{1,*} Soovin Lee,^{2,†} and M. S. Kim²

¹Quantum Research Center, Technology Innovation Institute, Abu Dhabi, UAE

²QOLS, Blackett Laboratory, Imperial College London SW7 2AZ, UK

(Dated: December 21, 2023)

Stabilizer entropies (SEs) are measures of nonstabilizerness or ‘magic’ that quantify the degree to which a state is described by stabilizers. SEs are especially interesting due to their connections to scrambling, localization and property testing. However, applications have been limited so far as previously known measurement protocols for SEs scale exponentially with the number of qubits. Here, we show how to efficiently measure SEs for integer index $n > 1$ via Bell measurements. We provide efficient bounds of various nonstabilizerness monotones which are intractable to compute beyond a few qubits. Using the IonQ quantum computer, we measure SEs of random Clifford circuits doped with non-Clifford gates and give bounds for the stabilizer fidelity, stabilizer extent and robustness of magic. As applications, we provide efficient algorithms to measure $4n$ -point out-of-time-order correlators and multifractal flatness. Our results open up the exploration of nonstabilizerness with quantum computers.

Stabilizer states and Clifford operations are essential to quantum information and quantum computing [1–3]. They are the cornerstone to run quantum algorithms on most fault-tolerant quantum computers, where Clifford operations are intertwined with non-Clifford gates [4, 5]. To characterize the amount of non-Clifford resources needed to realize quantum states and operations the resource theory of nonstabilizerness has been put forward [6–14]. Stabilizer entropies (SEs) [15] are measures of nonstabilizerness with efficient algorithms for matrix product states [16–18] which have enabled the study of nonstabilizerness in many-body systems [16–23].

Recently, SEs have also been related to various important properties of quantum systems. SEs probe error-correction [24] and measurement-induced phase transitions [25, 26], as well as relate to the entanglement spectrum [27] and property testing [28, 29]. SEs are also connected to the participation entropy [30], which are helpful to understand Anderson [31] and many-body localization [32]. Further, recent works established a fruitful connection between out-of-time-order correlators (OTOCs) and nonstabilizerness [29, 33, 34]. OTOCs describe scrambling in quantum systems [35, 36]. However, OTOCs are challenging to measure directly and often require an inverse of the time evolution [37]. Higher-order OTOCs and nonstabilizerness have been related to quantum chaos [33] and state certification [29].

The aforementioned properties make SEs highly interesting for experimental studies of quantum computers and simulators. However, the progress has so far been limited as all previously known measurement protocols for SEs scale exponentially with the number of qubits [14, 38].

Here, we show how to efficiently measure SEs with integer index $n > 1$ on quantum computers and simulators. Our algorithms are practical to implement via

Bell measurements over two copies of the state, where for even n we additionally require access to the complex conjugate of the state. We leverage the relationship between SEs and OTOCs to devise an efficient protocol for Pauli-averaged $4n$ -point OTOCs where for odd n we do not require an inverse time evolution. Further, we show how to measure the multifractal flatness. We provide efficiently computable bounds to other nonstabilizerness monotones, which are otherwise intractable beyond a few qubits. Finally, we measure the Tsallis SE on the IonQ quantum computer and demonstrate SEs as efficient bounds for the robustness of magic, stabilizer extent and stabilizer fidelity. Our work introduces methods to uncover the key features that characterize the power of quantum computers and simulators.

SE.— For an N -qubit state $|\psi\rangle$, the Rényi- n SE is given by [15]

$$M_n(|\psi\rangle) = (1 - n)^{-1} \ln \left(\sum_{\sigma \in \mathcal{P}} 2^{-N} \langle \psi | \sigma | \psi \rangle^{2n} \right). \quad (1)$$

where n is the index of the SE and \mathcal{P} is the set of 4^N Pauli strings. The Pauli strings are N -qubit tensor products $\sigma_{\mathbf{r}} = \bigotimes_{j=1}^N \sigma_{\mathbf{r}_{2j-1}\mathbf{r}_{2j}}$ with $\mathbf{r} \in \{0, 1\}^{2N}$ where $\sigma_{00} = I_1$, $\sigma_{01} = \sigma^x$, $\sigma_{10} = \sigma^z$ and $\sigma_{11} = \sigma^y$ with ℓ -qubit identity matrix I_ℓ and Pauli matrices σ^k , $k \in \{x, y, z\}$. M_n is a faithful measure of nonstabilizerness for pure states, i.e. $M_n(|\psi_{\text{STAB}}\rangle) = 0$ only for pure stabilizer states $|\psi_{\text{STAB}}\rangle$, and greater zero else [15]. Further, SEs are invariant under Clifford unitaries U_C with $M_n(U_C |\psi\rangle) = M_n(|\psi\rangle)$, where Clifford unitaries map any Pauli string σ to another Pauli string σ' via $U_C \sigma U_C^\dagger = \sigma'$. Further, M_n is additive with $M_n(|\psi\rangle \otimes |\phi\rangle) = M_n(|\psi\rangle) + M_n(|\phi\rangle)$. M_n for $n < 2$ is not a monotone under channels that can map a pure state to another pure state, while the case $n \geq 2$ remains an open problem.

Evaluating Eq. (1) requires an efficient measurement protocol for the n -th moment of the Pauli spectrum

$$A_n(|\psi\rangle) = 2^{-N} \sum_{\sigma \in \mathcal{P}} \langle \psi | \sigma | \psi \rangle^{2n}, \quad (2)$$

* tobias.haug@u.nus.edu

† soovinlee310@gmail.com

which on first glance appears challenging due to the summation over exponentially many Pauli strings.

Algorithms.— We now provide two algorithms to efficiently measure $A_n(|\psi\rangle)$. First, we introduce Algorithm 1 which is efficient for odd $n > 1$. We write A_n as the expectation value of an observable $\Gamma_n^{\otimes N}$ acting on $2n$ copies of $|\psi\rangle$ via the replica trick [16]

$$A_n = 2^{-N} \sum_{\sigma \in \mathcal{P}} \langle \psi | \sigma | \psi \rangle^{2n} = \langle \psi |^{\otimes 2n} \Gamma_n^{\otimes N} | \psi \rangle^{\otimes 2n}, \quad (3)$$

where $\Gamma_n = \frac{1}{2} \sum_{k=0}^3 (\sigma^k)^{\otimes 2n}$. For even $n > 1$, $2^{-N} \Gamma_n^{\otimes N}$ is a projector with two possible eigenvalues $\omega \in \{0, 2^N\}$ as shown in SM A. In contrast, for odd $n > 1$ it is unitary and hermitian with eigenvalues $\omega \in \{-1, 1\}$. This fact was previously pointed out in Ref. [39] for stabilizer testing.

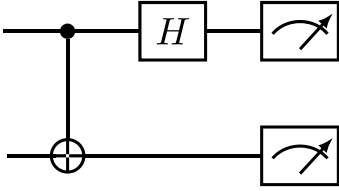


Figure 1. Bell measurement on two qubits.

To measure the operator $\Gamma_n^{\otimes N}$ we transform the operator into a diagonal eigenbasis. We first recall the Bell transformation (Fig. 1) acting on two qubits $U_{\text{Bell}} = (H \otimes I_1) \text{CNOT}$, where $H = \frac{1}{\sqrt{2}}(\sigma^x + \sigma^z)$ is the Hadamard gate, and $\text{CNOT} = \exp(i\frac{\pi}{4}(I_1 - \sigma^z) \otimes (I_1 - \sigma^x))$. It turns out Γ_n is diagonalized by U_{Bell}

$$A_n = \langle \psi |^{\otimes 2n} (U_{\text{Bell}}^{\otimes n} \dagger \frac{1}{2} ((I_1 \otimes I_1)^{\otimes n} + (\sigma^z \otimes I_1)^{\otimes n} + (I_1 \otimes \sigma^z)^{\otimes n} + (-1)^n (\sigma^z \otimes \sigma^z)^{\otimes n}) U_{\text{Bell}}^{\otimes n} | \psi \rangle^{\otimes 2n}. \quad (4)$$

Algorithm 1 utilizes this fact to provide an unbiased estimator for A_n , where \oplus denotes binary addition. While Eq. (4) involves $2n$ copies of $|\psi\rangle$, the Bell transformation Eq. (4) can be written as tensor products. Thus, A_n can be evaluated using only Bell measurements on two copies with a $2N$ -qubit quantum computer. A_n is then computed via post-processing by checking the parity of odd and even index qubits as derived in SM B.

We bound the maximal number L of measurement steps needed to measure SE with Hoeffding's inequality. The failure probability Δ to get an error ϵ between expectation value A_n and estimation \hat{A}_n is given by

$$P(|\hat{A}_n - A_n| \geq \epsilon) = \delta \leq 2 \exp\left(-\frac{2\epsilon^2 L}{\Delta\omega_n^2}\right), \quad (5)$$

where $\Delta\omega_n$ is the range of eigenvalues of $\Gamma_n^{\otimes N}$. To estimate A_n within ϵ accuracy and δ failure probability we require at most

$$L \leq \frac{\Delta\omega_n^2}{2\epsilon^2} \log\left(\frac{2}{\delta}\right) \quad (6)$$

measurement steps. For odd $n > 1$, we have $\Delta\omega_n = 2$ and the number of copies of $|\psi\rangle$ scales as $C = O(n\epsilon^{-2})$. For even n , the eigenvalue spectrum of $\Gamma_n^{\otimes N}$ diverges and Algorithm 1 requires in general an exponential number of measurements.

Algorithm 1: SE without complex conjugate

Input : Integer $n > 1$; L repetitions;
State preparation routine for $|\psi\rangle$
Output: $A_n(|\psi\rangle)$

```

1  $A_n = 0$ 
2 for  $k = 1, \dots, L$  do
3   for  $j = 1, \dots, n$  do
4     Prepare  $|\eta\rangle = U_{\text{Bell}}^{\otimes n} |\psi\rangle \otimes |\psi\rangle$ 
5     Sample in computational basis  $\mathbf{r}^{(j)} \sim |\langle \mathbf{r} | \eta \rangle|^2$ 
6   end
7    $b = 1$ 
8   for  $\ell = 1, \dots, N$  do
9      $\nu_1 = \bigoplus_{j=1}^n r_{2\ell-1}^{(j)}$ ;  $\nu_2 = \bigoplus_{j=1}^n r_{2\ell}^{(j)}$ 
10    if  $n$  is odd then
11       $b = b \cdot (-2\nu_1 \cdot \nu_2 + 1)$ 
12    else
13       $b = b \cdot 2(\nu_1 - 1) \cdot (\nu_2 - 1)$ 
14    end
15  end
16   $A_n = A_n + b/L$ 
17 end

```

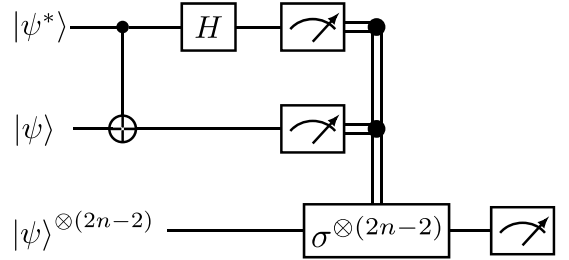


Figure 2. Measurement protocol for Algorithm 2.

Now, we provide Algorithm 2 which is efficient for any integer $n > 1$, however requires access to the complex conjugate $|\psi^*\rangle$. We rewrite the SE as a sampling problem

$$A_n = \mathbb{E}_{\sigma \sim \Xi(\sigma)} [\langle \psi | \sigma | \psi \rangle^{2n-2}], \quad (7)$$

where $\Xi(\sigma) = 2^{-N} \langle \psi | \sigma | \psi \rangle^2$ is the probability distribution of Pauli strings σ . The circuit for the algorithm is shown in Fig.2. First, we prepare $|\psi^*\rangle \otimes |\psi\rangle$ on the quantum computer and transform into the Bell basis $|\eta\rangle = U_{\text{Bell}}^{\otimes n} |\psi^*\rangle \otimes |\psi\rangle$. Next, we sample from $2N$ -qubit state $|\eta\rangle$ in the computational basis, gaining outcome $\mathbf{r} \in \{0, 1\}^{2N}$. As shown in [40, 41], we have $\Xi(\sigma_{\mathbf{r}}) = |\langle \mathbf{r} | \eta \rangle|^2$ where $|\mathbf{r}\rangle$ is the computational basis state corresponding to bitstring \mathbf{r} . Thus, sampling \mathbf{r} from $|\eta\rangle$ corresponds to sampling Pauli strings $\sigma_{\mathbf{r}} \sim \Xi(\sigma_{\mathbf{r}})$. Then, we perform $2n - 2$ measurements on $|\psi\rangle$ in the eigenbasis of the

Algorithm 2: SE with complex conjugate

Input : Integer $n > 1$; L repetitions;
 State preparation routines for $|\psi\rangle$ and $|\psi^*\rangle$

Output: $A_n(|\psi\rangle)$

```

1  $A_n = 0$ 
2 for  $k = 1, \dots, L$  do
3   Prepare  $|\eta\rangle = U_{\text{Bell}}^{\otimes N} |\psi^*\rangle \otimes |\psi\rangle$ 
4   Sample  $\mathbf{r} \sim |\langle \mathbf{r} | \eta \rangle|^2$ 
5    $b = 1$ 
6   for  $\ell = 1, \dots, 2n - 2$  do
7     Prepare  $|\psi\rangle$  and measure in eigenbasis of
       Paulistring  $\sigma_{\mathbf{r}}$  for eigenvalue  $\lambda \in \{+1, -1\}$ 
8      $b = b \cdot \lambda$ 
9   end
10   $A_n = A_n + b/L$ 
11 end

```

sampled $\sigma_{\mathbf{r}}$ and multiply the measured eigenvalues λ_k , gaining an unbiased estimator of $\langle \psi | \sigma_{\mathbf{r}} | \psi \rangle^{2n-2}$.

The number of repetitions L needed to gain accuracy ϵ with maximal failure probability δ is upper bounded by Eq. (5). The measured eigenvalues $\prod_{k=1}^{2n-2} \lambda_k \in \{+1, -1\}$ have a range $\Delta\omega_n = 2$, thus we require at most $C = O(n\epsilon^{-2})$ copies of $|\psi\rangle$ and $O(\epsilon^{-2})$ copies of $|\psi^*\rangle$ for any integer $n > 1$. Note that $|\psi^*\rangle$ cannot be efficiently prepared in general with only black-box access to $|\psi\rangle$ [42–44]. However, when we have a circuit description of the unitary preparing the state, $|\psi^*\rangle$ is constructed by an element-wise conjugation of the coefficients of the unitary [45].

Note that we can also efficiently compute gradients of A_n for parameterized quantum circuits via the shift-rule for variational quantum algorithms (see SM C).

Tsallis SE.— We now define a measure of nonstabilizerness which we call the Tsallis- n SE [46]

$$T_n(|\psi\rangle) = -(1-n)^{-1} \left(1 - \sum_{\sigma \in \mathcal{P}} 2^{-N} \langle \psi | \sigma | \psi \rangle^{2n}\right). \quad (8)$$

It is a generalization of the linear SE T_2 [15] and the von-Neumann SE $T_1 = M_1 = -2^{-N} \sum_{\sigma \in \mathcal{P}} \langle \psi | \sigma | \psi \rangle^2 \ln(\langle \psi | \sigma | \psi \rangle^2)$ [17]. T_n can be efficiently measured for integer $n > 1$ using our protocols. We have a direct relationship with the Rényi SE via $M_n = (1-n)^{-1} \ln(1 + (1-n)T_n)$ which makes it a faithful measure of nonstabilizerness which is invariant under Clifford unitaries. It lacks the additivity property of the Rényi SE. However, the Tsallis SEs may be a strong monotone which is a not necessary but highly desirable property for resource measures [47]. We have numerical evidence that the Tsallis- n SE is a strong monotone for $n \geq 2$, while n -Rényi SEs are not strong monotones for any n (see SM D) [17].

Note that measuring the Rényi SE $M_n \sim \ln(A_n)$ with precision ϵ_M requires $O(n \exp(M_n) \epsilon_M^{-2})$ samples due to the logarithm (see SM D). Thus, M_n is efficiently measurable as long as $M_n = O(\log(N))$.

Pauli-averaged OTOCs.— We now efficiently measure

the $4n$ -point OTOC averaged over all Pauli strings for N -qubit unitaries U and $n > 1$. The $4n$ -point OTOC for N -qubit Pauli strings σ and σ' is given by [29]

$$\begin{aligned} \text{otoc}_{4n}(U, \sigma, \sigma') &= (2^{-N} \text{tr}(\sigma U \sigma' U^\dagger))^{2n} \\ &= 2^{-N} \text{tr}(\langle \sigma^{(2n)} \prod_{i=1}^{2n} (U \sigma U^\dagger \sigma' \sigma^{(i-1)} \sigma^{(i)}) \rangle_{\sigma^{(1)}, \dots, \sigma^{(2n)}}), \end{aligned} \quad (9)$$

where $\sigma^{(0)} = I_N$ and $\langle X \rangle_{\sigma^{(1)}, \sigma^{(2)}, \dots, \sigma^{(2n)}} = 4^{-2nN} \sum_{\sigma^{(1)}, \dots, \sigma^{(2n)} \in \mathcal{P}} X$ denotes the average over the Pauli strings $\sigma^{(1)}, \dots, \sigma^{(2n)}$. We now regard the $4n$ -point OTOC averaged over all Pauli strings σ, σ' [29]

$$\text{OTOC}_{4n}(U) = 4^{-N} \sum_{\sigma, \sigma' \in \mathcal{P}} \text{otoc}_{4n}(U, \sigma, \sigma'). \quad (10)$$

This quantity describes the average OTOCs over both local and global Pauli strings. Alternatively, Eq. (10) can be interpreted as the $4n$ -point OTOC for a fixed σ, σ' but where the unitary $U \rightarrow U_C U U'_C$ is averaged over random Clifford unitaries U_C, U'_C . We now recall the Choi state $|U\rangle = I_N \otimes U |\Phi\rangle$, where $|\Phi\rangle = 2^{-N/2} \sum_{i=0}^{2^N-1} |i\rangle \otimes |i\rangle$ is the maximally entangled state and $|i\rangle$ are the computational basis states. Using the relationship between OTOC and Rényi SE derived in Ref. [29], we find

$$\text{OTOC}_{4n}(U) = A_n(|U\rangle). \quad (11)$$

For odd n , we can efficiently measure $\text{OTOC}_{4n}(U)$ via Algorithm 1 alongside the preparation of Choi state $|U\rangle$. For even n , we additionally require the complex conjugate $|U^*\rangle$ for Algorithm 2. The complex conjugate of the Choi state can be efficiently prepared as long as one has access to either U^* or U^\dagger due to the ricochet property $|U^*\rangle = I_N \otimes U^* |\Phi\rangle = U^{*\text{T}} \otimes I |\Phi\rangle = U^\dagger \otimes I_N |\Phi\rangle$ [45].

Participation entropy.— The participation entropy is given by $\mathcal{I}_q(|\psi\rangle) = \sum_k |\langle k | \psi \rangle|^{2q}$ where $|k\rangle$ are computational basis states, $q > 0$ and $0 \leq \mathcal{I}_q \leq 1$ [31]. The participation entropy quantifies the spread of the wavefunction over basis states, i.e. $\mathcal{I}_q = 1$ for computational basis states, while it is small when the state is delocalized over many computational basis states. The multifractal flatness $\mathcal{F}(|\psi\rangle) = \mathcal{I}_3(|\psi\rangle) - \mathcal{I}_2^2(|\psi\rangle)$ measures the flatness of the distribution $|\langle k | \psi \rangle|^2$, i.e. we have $\mathcal{F} = 0$ when the distribution $|\langle k | \psi \rangle|^2$ is constant over its support, else we have $\mathcal{F} > 0$. In particular, stabilizer states have $\mathcal{F} = 0$ [48].

Recently, \mathcal{F} averaged over the group of Clifford unitaries \mathcal{C} has been proposed as $\bar{\mathcal{F}}$ [30]. This quantity describes the participation ratio averaged over all possible choices of basis states. $\bar{\mathcal{F}}$ has been connected to SEs as follows [30]

$$\bar{\mathcal{F}}(|\psi\rangle) = \mathbb{E}_{U_C \in \mathcal{C}} [\mathcal{F}(U_C |\psi\rangle)] = \frac{2(1 - A_n(|\psi\rangle))}{(2^N + 1)(2^N + 2)}. \quad (12)$$

Thus, Algorithm 2 allows us to efficiently measure $\bar{\mathcal{F}}(|\psi\rangle)$ which otherwise is difficult to measure directly as $\bar{\mathcal{F}}$ is an exponentially small quantity.

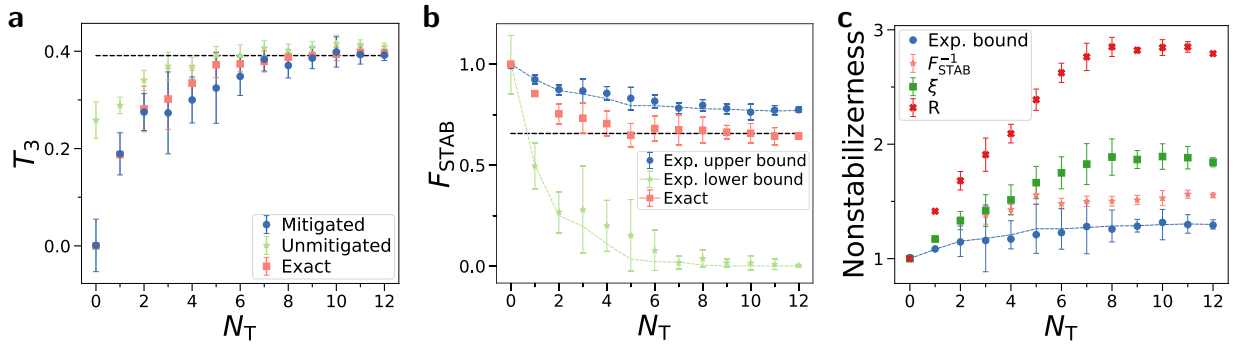


Figure 3. Measurement of nonstabilizerness for quantum states generated by Eq. (15) with random Clifford circuits doped with N_T T-gates on the IonQ quantum computer. **a)** We show Tsallis SE T_3 with and without error mitigation as well as exact simulation. Dashed line is average value for Haar random states. Dots represent mean value and error bars the standard deviation taken over 6 random instances of the circuit. We have $N = 3$ qubits, 10^3 Bell measurements and a measured depolarization error of $p \approx 0.1$. **b)** We show upper and lower bounds on F_{STAB} via Eq. (14) evaluated using the error mitigated T_3 as blue and green dots as well as simulation of the bound as dashed lines. The orange dots show simulations of F_{STAB} . **c)** We demonstrate the hierarchy of bounds Eq. (13) for different measures of nonstabilizerness using error mitigated A_3 as well as simulations of F_{STAB}^{-1} , stabilizer extent ξ and robustness of magic R .

Bounds on nonstabilizerness.— We now provide efficient bounds on three magic monotones, namely the robustness of magic R [8], stabilizer extent ξ [49] and the stabilizer fidelity $F_{\text{STAB}} = \max_{|\phi\rangle \in \text{STAB}} |\langle \psi | \phi \rangle|^2$ [49] (see SM E). Computing R , ξ and F_{STAB} requires solving an optimization program over the set of pure N -qubit stabilizer states. As the number of stabilizer states scales as $O(2^{N^2})$, these three measures in general become numerically infeasible beyond 5 qubits [8, 50].

Our algorithms provide efficient bounds for integer $n > 1$ (see [17] or SM E):

$$R \geq \xi \geq F_{\text{STAB}}^{-1} \geq A_n^{-\frac{1}{2n}}. \quad (13)$$

The bound can be tightened for $n \geq \frac{1}{2}$ to $R \geq A_n^{\frac{1}{2(1-n)}}$ [8, 15]. With methods from Ref. [39, 51], we also prove a lower bound on F_{STAB} for $n > 1$ (see SM F)

$$A_n^{\frac{1}{2n}} \geq F_{\text{STAB}} \geq \frac{A_n - 2^{1-n}}{1 - 2^{1-n}}. \quad (14)$$

The min-relative entropy of magic $D_{\min} = -\ln(F_{\text{STAB}})$ can be seen as the distance to the nearest stabilizer state. We now argue that D_{\min} , Rényi SEs with $n \geq 2$ and the recently introduced additive Bell magic \mathcal{B}_a [14] are closely related. In particular, we find evidence for respective upper and lower bounds independent of qubit number N (see SM G). Via numerical optimization we find $1.7M_2 \gtrsim D_{\min} \geq \frac{1}{4}M_2$ as well as $3.5M_2 \gtrsim \mathcal{B}_a \gtrsim 2.88M_2$ for at least $N \leq 4$, while similar bounds can also be found for larger n . Thus, D_{\min} , $M_{n \geq 2}$ and \mathcal{B}_a can be seen as measures of nonstabilizerness that relate to the distance to the nearest stabilizer state. In contrast, the robustness of magic R and stabilizer extent ξ relate to the degree a state can be approximated by a combination of stabilizer states. They belong to a different class of nonstabilizerness measures as they cannot be upper bounded with D_{\min} or M_n for $n > 1/2$ [17].

Demonstration.— We now study the Tsallis SE with Bell measurements on the IonQ quantum computer [14] using Algorithm 1 in Fig. 3. We investigate the SE of random Clifford circuits U_C doped with N_T non-Clifford gates

$$|\psi(N_T)\rangle = U_C^{(0)} \prod_{k=1}^{N_T} V_T^{(k)} U_C^{(k)} |0\rangle, \quad (15)$$

where $V_T^{(k)} = \exp(-i\frac{\pi}{8}\sigma_{g(k)}^z)$ is the T-gate of the k -th layer acting on a randomly chosen qubit $g(k)$. With increasing N_T these states transition from efficiently simulable stabilizer states to intractable quantum states [33, 52]. To reduce noise, we compress the circuits into layered circuits composed of single-qubit operations and CNOT gates arranged in a nearest-neighbor chain configuration [14]. The state prepared by the quantum computer is not pure but degraded by noise. However, SEs are faithful measures of nonstabilizerness only for pure states. Using measurements on the noisy state, we mitigate A_n and T_n from measurements on noisy states by assuming a global depolarization error model (see SM H).

In Fig. 3a, we show T_3 with and without error mitigation for different N_T , where for each value we average over 6 random instances of Eq. (15). We find that the results on the IonQ quantum computer with error mitigation closely match the simulated values. The Tsallis SE is zero for $N_T = 0$, then increases with N_T until it converges to the average value of Haar random states indicated as black dashed line. In Fig. 3b, we use the mitigated results for A_3 to compute upper and lower bounds for the stabilizer fidelity F_{STAB} using Eq. (14). The measured result indeed gives valid bounds of the exactly simulated F_{STAB} . We find that the upper bound is relatively tight, while the lower bound is non-trivial only for small N_T . In Fig. 3c, we demonstrate the hierarchy of bounds between

the measures of nonstabilizerness according to Eq. (13). In SM I, we provide additional results for the IonQ quantum computer on measures of nonstabilizerness. While our error mitigation scheme assumes global depolarization noise, we find that it works well even on actual quantum computers which have more complicated noise profiles. In SM J, we simulate our error mitigation scheme for various unital and non-unital noise models, and find very good performance. As SEs are moments of exponentially many Pauli strings, we believe self-averaging effects may explain the good performance of our scheme.

Discussions.— We show how to efficiently measure SEs with a cost independent of qubit number N , which is an exponential improvement over previous protocols [14, 38]. For integer $n > 1$, our protocol is asymptotically optimal with the number of copies scaling as $O(n\epsilon^{-2})$ and the classical post-processing time as $O(nN\epsilon^{-2})$. The protocol is easy to implement using Bell measurements which have been demonstrated for quantum computers and simulators [53–55]. We note that our approach is distinct from the previously introduced Bell magic as we show in SM K [14].

Our measurement protocol allows for efficient experimental characterization of different important properties of quantum states. We demonstrate an efficient bound on nonstabilizerness monotones which otherwise are hard to compute beyond a few qubits. These monotones serve as lower bounds on state preparation complexity and characterize the runtime of classical simulation algorithms [8, 49]. Further, we show how to efficiently measure a class of $4n$ -point OTOCs. Our protocol has the advantage that it does not require implementing

time-reversal for odd $n > 1$ which can be a challenge [35]. Our protocol can measure higher order OTOCs which promise to reveal more features compared to the usually considered 4-point OTOCs [56, 57]. We also give an efficient protocol to evaluate multifractal flatness which characterizes the distribution of basis states of wavefunctions. Finally, our work enables the experimental study of phase transitions in SE which have been found for purity testing [28] and quantum error correction [24], as well as characterization of recent experiments on fault-tolerant encodings of magic states [58, 59].

Future work could find efficient protocols for even n without the need of complex conjugation, prove or refute the strong monotonicity condition for the Tsallis SE for $n \geq 2$, and tighten the lower bound of SE for the stabilizer fidelity.

The code for this work is available on Github [60].

Acknowledgments

Acknowledgements.— We thank Hyukjoon Kwon, Ludovico Lami, Lorenzo Leone, Salvatore F.E. Oliviero, Adam Taylor and especially Lorenzo Piroli for inspiring discussions. We thank IonQ for providing quantum computing resources. This work is supported by a Samsung GRC project and the UK Hub in Quantum Computing and Simulation, part of the UK National Quantum Technologies Programme with funding from UKRI EPSRC grant EP/T001062/1.

-
- [1] Daniel Gottesman, *Stabilizer codes and quantum error correction*. *Caltech Ph. D.*, Ph.D. thesis, Thesis, eprint: quant-ph/9705052 (1997).
 - [2] Peter W Shor, “Fault-tolerant quantum computation,” in *Proceedings of 37th conference on foundations of computer science* (IEEE, 1996) pp. 56–65.
 - [3] A Yu Kitaev, “Fault-tolerant quantum computation by anyons,” *Ann. Phys.* **303**, 2–30 (2003).
 - [4] Sergey Bravyi and Alexei Kitaev, “Universal quantum computation with ideal clifford gates and noisy ancillas,” *Phys. Rev. A* **71**, 022316 (2005).
 - [5] Earl T Campbell, Barbara M Terhal, and Christophe Vuillot, “Roads towards fault-tolerant universal quantum computation,” *Nature* **549**, 172–179 (2017).
 - [6] Earl T. Campbell, “Catalysis and activation of magic states in fault-tolerant architectures,” *Phys. Rev. A* **83**, 032317 (2011).
 - [7] Victor Veitch, SA Hamed Mousavian, Daniel Gottesman, and Joseph Emerson, “The resource theory of stabilizer quantum computation,” *New J. Phys.* **16**, 013009 (2014).
 - [8] Mark Howard and Earl Campbell, “Application of a resource theory for magic states to fault-tolerant quantum computing,” *Phys. Rev. Lett.* **118**, 090501 (2017).
 - [9] Xin Wang, Mark M Wilde, and Yuan Su, “Quantifying the magic of quantum channels,” *New J. Phys.* **21**, 103002 (2019).
 - [10] Michael Beverland, Earl Campbell, Mark Howard, and Vadym Kliuchnikov, “Lower bounds on the non-clifford resources for quantum computations,” *Quantum Science Tech.* **5**, 035009 (2020).
 - [11] Jiaqing Jiang and Xin Wang, “Lower bound for the t count via unitary stabilizer nullity,” *Physical Review Applied* **19**, 034052 (2023).
 - [12] Zi-Wen Liu and Andreas Winter, “Many-body quantum magic,” *PRX Quantum* **3**, 020333 (2022).
 - [13] Kaifeng Bu, Roy J Garcia, Arthur Jaffe, Dax Enshan Koh, and Lu Li, “Complexity of quantum circuits via sensitivity, magic, and coherence,” *arXiv:2204.12051* (2022).
 - [14] Tobias Haug and M.S. Kim, “Scalable measures of magic resource for quantum computers,” *PRX Quantum* **4**, 010301 (2023).
 - [15] Lorenzo Leone, Salvatore F. E. Oliviero, and Alioscia Hamma, “Stabilizer rényi entropy,” *Phys. Rev. Lett.* **128**, 050402 (2022).
 - [16] Tobias Haug and Lorenzo Piroli, “Quantifying nonstabilizerness of matrix product states,” *Phys. Rev. B* **107**, 035148 (2023).
 - [17] Tobias Haug and Lorenzo Piroli, “Stabilizer entropies and nonstabilizerness monotones,” *Quantum* **7**, 1092

- (2023).
- [18] Guglielmo Lami and Mario Collura, “Nonstabilizerness via perfect pauli sampling of matrix product states,” *Phys. Rev. Lett.* **131**, 180401 (2023).
- [19] Salvatore F. E. Oliviero, Lorenzo Leone, and Alioscia Hamma, “Magic-state resource theory for the ground state of the transverse-field ising model,” *Phys. Rev. A* **106**, 042426 (2022).
- [20] Jovan Odavić, Tobias Haug, Gianpaolo Torre, Alioscia Hamma, Fabio Franchini, and Salvatore Marco Gimpaolo, “Complexity of frustration: a new source of non-local non-stabilizerness,” *SciPost Physics* **15**, 131 (2023).
- [21] Liyuan Chen, Roy J Garcia, Kaifeng Bu, and Arthur Jaffe, “Magic of random matrix product states,” [arXiv:2211.10350](https://arxiv.org/abs/2211.10350) (2022).
- [22] Kanato Goto, Tomoki Nosaka, and Masahiro Nozaki, “Probing chaos by magic monotones,” *Physical Review D* **106**, 126009 (2022).
- [23] Stefano Piemontese, Tommaso Roscilde, and Alioscia Hamma, “Entanglement complexity of the rokhsarkivelson-sign wavefunctions,” *Physical Review B* **107**, 134202 (2023).
- [24] Pradeep Niroula, Christopher David White, Qingfeng Wang, Sonika Johri, Daiwei Zhu, Christopher Monroe, Crystal Noel, and Michael J. Gullans, “Phase transition in magic with random quantum circuits,” [arXiv:2304.10481](https://arxiv.org/abs/2304.10481) (2023).
- [25] M. Bejan, C. McLauchlan, and B. Béri, “Dynamical magic transitions in monitored clifford+t circuits,” [arXiv:2312.00132](https://arxiv.org/abs/2312.00132) (2023).
- [26] Gerald E. Fux, Emanuele Tirrito, Marcello Dalmonte, and Rosario Fazio, “Entanglement-magic separation in hybrid quantum circuits,” [arXiv:2312.02039](https://arxiv.org/abs/2312.02039) (2023).
- [27] Emanuele Tirrito, Poetri Sonya Tarabunga, Guglielmo Lami, Titas Chanda, Lorenzo Leone, Salvatore F. E. Oliviero, Marcello Dalmonte, Mario Collura, and Alioscia Hamma, “Quantifying non-stabilizerness through entanglement spectrum flatness,” [arXiv preprint arXiv:2304.01175](https://arxiv.org/abs/2304.01175) (2023).
- [28] Lorenzo Leone, Salvatore F. E. Oliviero, Gianluca Esposito, and Alioscia Hamma, “Phase transition in stabilizer entropy and efficient purity estimation,” [arXiv:2302.07895](https://arxiv.org/abs/2302.07895) (2023).
- [29] Lorenzo Leone, Salvatore F. E. Oliviero, and Alioscia Hamma, “Nonstabilizerness determining the hardness of direct fidelity estimation,” *Phys. Rev. A* **107**, 022429 (2023).
- [30] Xhek Turkeshi, Marco Schirò, and Piotr Sierant, “Measuring nonstabilizerness via multifractal flatness,” *Phys. Rev. A* **108**, 042408 (2023).
- [31] C Castellani and L Peliti, “Multifractal wavefunction at the localisation threshold,” *Journal of physics A: mathematical and general* **19**, L429 (1986).
- [32] Jean-Marie Stéphan, Shunsuke Furukawa, Grégoire Misguich, and Vincent Pasquier, “Shannon and entanglement entropies of one-and two-dimensional critical wave functions,” *Physical Review B* **80**, 184421 (2009).
- [33] Lorenzo Leone, Salvatore F. E. Oliviero, You Zhou, and Alioscia Hamma, “Quantum chaos is quantum,” *Quantum* **5**, 453 (2021).
- [34] Roy J Garcia, Kaifeng Bu, and Arthur Jaffe, “Resource theory of quantum scrambling,” *Proceedings of the National Academy of Sciences* **120**, e2217031120 (2023).
- [35] Shenglong Xu and Brian Swingle, “Scrambling dynamics and out-of-time ordered correlators in quantum many-body systems: a tutorial,” [arXiv:2202.07060](https://arxiv.org/abs/2202.07060) (2022).
- [36] Neil Dowling, Pavel Kos, and Kavan Modi, “Scrambling is necessary but not sufficient for chaos,” [arXiv:2304.07319](https://arxiv.org/abs/2304.07319) (2023).
- [37] Jun Li, Ruihua Fan, Hengyan Wang, Bingtian Ye, Bei Zeng, Hui Zhai, Xinhua Peng, and Jiangfeng Du, “Measuring out-of-time-order correlators on a nuclear magnetic resonance quantum simulator,” *Physical Review X* **7**, 031011 (2017).
- [38] Salvatore F. E. Oliviero, Lorenzo Leone, Alioscia Hamma, and Seth Lloyd, “Measuring magic on a quantum processor,” *npj Quantum Information* **8**, 148 (2022).
- [39] David Gross, Sepehr Nezami, and Michael Walter, “Schur–weyl duality for the clifford group with applications: Property testing, a robust hudson theorem, and de finetti representations,” *Communications in Mathematical Physics* **385**, 1325–1393 (2021).
- [40] Ashley Montanaro, “Learning stabilizer states by bell sampling,” [arXiv:1707.04012](https://arxiv.org/abs/1707.04012) (2017).
- [41] Ching-Yi Lai and Hao-Chung Cheng, “Learning quantum circuits of some t gates,” *IEEE Transactions on Information Theory* **68**, 3951–3964 (2022).
- [42] Yuxiang Yang, Giulio Chiribella, and Gerardo Adesso, “Certifying quantumness: Benchmarks for the optimal processing of generalized coherent and squeezed states,” *Physical Review A* **90**, 042319 (2014).
- [43] Jisho Miyazaki, Akihito Soeda, and Mio Muraio, “Complex conjugation supermap of unitary quantum maps and its universal implementation protocol,” *Physical Review Research* **1**, 013007 (2019).
- [44] Tobias Haug, Kishor Bharti, and Dax Enshan Koh, “Pseudorandom unitaries are neither real nor sparse nor noise-robust,” [arXiv:2306.11677](https://arxiv.org/abs/2306.11677) (2023).
- [45] Sumeet Khatri, Ryan LaRose, Alexander Poremba, Lukasz Cincio, Andrew T Sornborger, and Patrick J Coles, “Quantum-assisted quantum compiling,” *Quantum* **3**, 140 (2019).
- [46] Constantino Tsallis, “Possible generalization of boltzmann-gibbs statistics,” *Journal of statistical physics* **52**, 479–487 (1988).
- [47] Eric Chitambar and Gilad Gour, “Quantum resource theories,” *Rev. Mod. Phys.* **91**, 025001 (2019).
- [48] Piotr Sierant and Xhek Turkeshi, “Universal behavior beyond multifractality of wave functions at measurement-induced phase transitions,” *Physical Review Letters* **128**, 130605 (2022).
- [49] Sergey Bravyi, Dan Browne, Padraic Calpin, Earl Campbell, David Gosset, and Mark Howard, “Simulation of quantum circuits by low-rank stabilizer decompositions,” *Quantum* **3**, 181 (2019).
- [50] Scott Aaronson and Daniel Gottesman, “Improved simulation of stabilizer circuits,” *Phys. Rev. A* **70**, 052328 (2004).
- [51] Sabee Grewal, Vishnu Iyer, William Kretschmer, and Daniel Liang, “Improved stabilizer estimation via bell difference sampling,” [arXiv:2304.13915](https://arxiv.org/abs/2304.13915) (2023).
- [52] Jonas Haferkamp, “Random quantum circuits are approximate unitary t -designs in depth $o(nt^{5+o(1)})$,” *Quantum* **6**, 795 (2022).
- [53] Rajibul Islam, Ruichao Ma, Philipp M Preiss, M Eric Tai, Alexander Lukin, Matthew Rispoli, and Markus

- Greiner, “Measuring entanglement entropy in a quantum many-body system,” *Nature* **528**, 77–83 (2015).
- [54] Hsin-Yuan Huang, Michael Broughton, Jordan Cotler, Sitan Chen, Jerry Li, Masoud Mohseni, Hartmut Neven, Ryan Babbush, Richard Kueng, John Preskill, *et al.*, “Quantum advantage in learning from experiments,” *Science* **376**, 1182–1186 (2022).
- [55] Dolev Bluvstein, Harry Levine, Giulia Semeghini, Tout T Wang, Sepehr Ebadi, Marcin Kalinowski, Alexander Keesling, Nishad Maskara, Hannes Pichler, Markus Greiner, *et al.*, “A quantum processor based on coherent transport of entangled atom arrays,” *Nature* **604**, 451–456 (2022).
- [56] Daniel A Roberts and Beni Yoshida, “Chaos and complexity by design,” *Journal of High Energy Physics* **2017**, 1–64 (2017).
- [57] Roy J Garcia, You Zhou, and Arthur Jaffe, “Quantum scrambling with classical shadows,” *Physical Review Research* **3**, 033155 (2021).
- [58] Yangsen Ye, Tan He, He-Liang Huang, Zuolin Wei, Yiming Zhang, Youwei Zhao, Dachao Wu, Qingling Zhu, Huijie Guan, Sirui Cao, Fusheng Chen, Tung-Hsun Chung, Hui Deng, Daojin Fan, Ming Gong, Cheng Guo, Shaojun Guo, Lianchen Han, Na Li, Shaowei Li, Yuan Li, Futtian Liang, Jin Lin, Haoran Qian, Hao Rong, Hong Su, Shiyu Wang, Yulin Wu, Yu Xu, Chong Ying, Jiale Yu, Chen Zha, Kaili Zhang, Yong-Heng Huo, Chao-Yang Lu, Cheng-Zhi Peng, Xiaobo Zhu, and Jian-Wei Pan, “Near-perfect logical magic state preparation on a superconducting quantum processor,” arXiv:2305.15972 (2023).
- [59] Riddhi S. Gupta, Neereja Sundaresan, Thomas Alexander, Christopher J. Wood, Seth T. Merkel, Michael B. Healy, Marius Hillenbrand, Tomas Jochym-O’Connor, James R. Wootton, Theodore J. Yoder, Andrew W. Cross, Maika Takita, and Benjamin J. Brown, “Encoding a magic state with beyond break-even fidelity,” arXiv:2305.13581 (2023).
- [60] Tobias Haug, “Code for measuring stabilizer entropy on quantum computers,” https://github.com/txhaug/stabilizer_entropy.
- [61] Kosuke Mitarai, Makoto Negoro, Masahiro Kitagawa, and Keisuke Fujii, “Quantum circuit learning,” *Physical Review A* **98**, 032309 (2018).
- [62] Juan Carlos Garcia-Escartin and Pedro Chamorro-Posada, “Swap test and hong-ou-mandel effect are equivalent,” *Physical Review A* **87**, 052330 (2013).

Supplemental Materials

We provide additional technical details and data supporting the claims in the main text.

Contents

A. Spectrum of SE observable	8
B. Parity check to evaluate SEs	9
C. Parameter-shift rule for gradient of SE	9
D. Strong monotonicity and measuring Rényi SEs	10
E. Other nonstabilizerness monotones and known bounds	12
F. Proof of lower bound of stabilizer fidelity	13
G. Relationship of measures of nonstabilizerness	13
H. Error mitigation	14
I. Further IonQ quantum computer results	14
J. Error mitigation for different noise models	15
K. Bell measurements, stabilizer entropy and Bell magic	17

Supplemental Materials A: Spectrum of SE observable

We now discuss the eigenvalue spectrum of the observable that measures the SE. The SE is defined as a sum over powers of expectation value of the Pauli operator. By assuming access to n copies, we can write it in terms of an SE observable

$$A_n = \sum_{\sigma \in \mathcal{P}} \frac{\langle \psi | \sigma | \psi \rangle^{2n}}{2^N} = \langle \psi |^{\otimes 2n} \Gamma_n^{\otimes N} | \psi \rangle^{\otimes 2n}, \quad (\text{S1})$$

where $\Gamma_n = \frac{1}{2} \sum_{\alpha=0}^3 (\sigma_\alpha)^{\otimes 2n}$. Using the definitions $\sigma_y = i\sigma_x\sigma_z$ and $(A \otimes B)(C \otimes D) = (AC) \otimes (BD)$, the following can be deduced:

$$\sigma_y^{\otimes 2n} = \begin{cases} +\sigma_x^{\otimes 2n} \sigma_z^{\otimes 2n} & : n = \text{even}, \\ -\sigma_x^{\otimes 2n} \sigma_z^{\otimes 2n} & : n = \text{odd}. \end{cases} \quad (\text{S2})$$

With the above considerations, Γ_n^2 can then be expanded in terms of I_1 , σ_x , and σ_z . Finally, consider the commutation relations of tensor-product Paulis $[\sigma_x^{\otimes 2n}, \sigma_z^{\otimes 2n}] = 0$ to simplify the expanded terms and realise, for $n \geq 2$,

$$\Gamma_n^2 = \begin{cases} 2\Gamma_n & : n = \text{even}, \\ I_{2n} & : n = \text{odd}. \end{cases} \quad (\text{S3})$$

For odd n , we have $\Gamma_n^2 = I_{2n}$. This implies that the eigenvalues of Γ_n must $\lambda = \pm 1$. Thus, the SE operator $A_n = \Gamma_n^{\otimes N}$ has the same eigenvalue spectrum $\lambda = \pm 1$. In contrast for even n , we have $\Gamma_n^2 = 2\Gamma_n$. One can check that the possible eigenvalues are $\lambda = 0$ and $\lambda = 2$. Thus, the spectrum of $\Gamma_n^{\otimes N}$ consists of eigenvalues $\lambda = 0$ and $\lambda = 2^N$.

Supplemental Materials B: Parity check to evaluate SEs

We now derive the parity check rules to evaluate A_n using Algorithm 1. To evaluate A_n , we note it is composed as a tensor product of N operators which we evaluate one by one with a simple rule. In particular, for the operator $U_{\text{Bell}}^{\otimes n} \Gamma_n U_{\text{Bell}}^{\otimes n \dagger}$ and the corresponding state $|\psi\rangle^{\otimes 2n}$, we reorder the position of the qubits $(r_1, r_2, \dots, r_{2n}) \rightarrow (r_1, r_3, \dots, r_{2n-1}, r_2, r_4, \dots, r_{2n})$ such that the odd-indexed qubits occupy the first half, and the even-indexed qubits the second half of the register. Then, we find for the transformed operator for odd n the simple form

$$[U_{\text{Bell}}^{\otimes n} \Gamma_n U_{\text{Bell}}^{\otimes n \dagger}]_{\text{reorder}} = -\frac{1}{2}(1 - \sigma^{z \otimes n}) \otimes (1 - \sigma^{z \otimes n}) + 1 \quad (\text{S1})$$

and for even n

$$[U_{\text{Bell}}^{\otimes n} \Gamma_n U_{\text{Bell}}^{\otimes n \dagger}]_{\text{reorder}} = \frac{1}{2}(1 + \sigma^{z \otimes n}) \otimes (1 + \sigma^{z \otimes n}). \quad (\text{S2})$$

Here, the expectation value $\langle x \rangle = \langle x | (1 - \sigma^{z \otimes n}) | x \rangle$ for n -dimensional computational basis state $|x\rangle$ is $\langle x \rangle = 2$ when x has odd parity, and 0 otherwise. In contrast, $\langle x | (1 + \sigma^{z \otimes n}) | x \rangle$ is 2 when x has even parity, and is 0 otherwise. Thus, we see that $U_{\text{Bell}}^{\otimes n} \Gamma_n U_{\text{Bell}}^{\otimes n \dagger}$ can be evaluated by checking the parity of the odd-indexed and even-indexed qubits.

Supplemental Materials C: Parameter-shift rule for gradient of SE

We now derive the parameter-shift rule for observables that act on multiple copies of a state. First, we regard the generator G of the unitary operator $\mathcal{G}(\mu) = e^{-i\mu G}$ has two distinct eigenvalues, we can shift the eigenvalues to $\pm r$. Note that any single qubit gate is of this form, which implies $G^2 = r^2 I$, where I is the identity matrix. The Taylor series of $\mathcal{G}(\mu)$ shows

$$\begin{aligned} \mathcal{G}(\mu) &= \exp(-i\mu G) = \sum_{k=0}^{\infty} \frac{(-i\mu)^k G^k}{k!} \\ &= \sum_{k=0}^{\infty} \frac{(-i\mu)^{2k} G^{2k}}{(2k)!} + \sum_{k=0}^{\infty} \frac{(-i\mu)^{2k+1} G^{2k+1}}{(2k+1)!} \\ &= I \sum_{k=0}^{\infty} \frac{(-1)^k (r\mu)^{2k}}{(2k)!} - ir^{-1} G \sum_{k=0}^{\infty} \frac{(-1)^k (r\mu)^{2k+1}}{(2k+1)!} \\ &= I \cos(r\mu) - ir^{-1} G \sin(r\mu). \end{aligned} \quad (\text{S1})$$

Thus the following identity holds

$$\mathcal{G}\left(\frac{\pi}{4r}\right) = \frac{1}{\sqrt{2}}(I - ir^{-1}G). \quad (\text{S2})$$

Now, we assume an N -qubit parameterized quantum circuit $|\psi\rangle \equiv |\psi(\boldsymbol{\theta})\rangle = \prod_{n=1}^d V_n(\boldsymbol{\theta}_n) W_n |0\rangle$ with d layers, entangling gates W_n , parameters $\boldsymbol{\theta}$ and parameterized rotations $V_n(\boldsymbol{\theta}_n) = e^{-i\frac{\boldsymbol{\theta}_n}{2} \cdot \boldsymbol{\sigma}_n}$ given by some Pauli strings $\boldsymbol{\sigma}_n$. For any operators U , O , and V we have

$$\langle \psi | U^\dagger O V | \psi \rangle + \text{h.c.} = \frac{1}{2} \left[\langle \psi | (U + V)^\dagger \hat{O} (U + V) | \psi \rangle - \langle \psi | (U - V)^\dagger \hat{O} (U - V) | \psi \rangle \right], \quad (\text{S3})$$

where h.c. is the hermitian conjugate of the preceding terms [61].

To measure SE, we calculate the expectation value

$$\langle O^{(K)}(\boldsymbol{\theta}) \rangle = \langle \psi(\boldsymbol{\theta}) |^{\otimes K} O^{(K)} | \psi(\boldsymbol{\theta}) \rangle^{\otimes K}, \quad (\text{S4})$$

over K copies of state $|\psi\rangle \in \mathbb{C}^{2^N}$ with in respect to an operator $O^{(K)} \in \mathbb{C}^{2^{NK}}$. For $K = 1$, i.e. measurements on a single quantum state, the shift rule is given by $\partial_k \langle O^{(1)}(\boldsymbol{\theta}) \rangle = \frac{1}{2} (\langle O^{(1)}(\boldsymbol{\theta} + \mathbf{e}_k \frac{\pi}{2}) \rangle - \langle O^{(1)}(\boldsymbol{\theta} - \mathbf{e}_k \frac{\pi}{2}) \rangle)$, where \mathbf{e}_k is the k th unit vector [61].

We now derive the shift-rule for general K . The derivative of the quantum state $|\psi\rangle$ is given by

$$\begin{aligned}\partial_k |\psi(\boldsymbol{\theta})\rangle &= \prod_{n=k+1}^d [V_n(\boldsymbol{\theta}_n) W_n] \left(-i\frac{1}{2}\sigma_k\right) \prod_{n=1}^k [V_n(\boldsymbol{\theta}_n) W_n] |0\rangle \\ &\equiv U_k \left(-i\frac{1}{2}\sigma_k\right) |\phi_k\rangle,\end{aligned}\tag{S5}$$

where $U_k = \prod_{n=k+1}^d [V_n(\boldsymbol{\theta}_n) W_n]$ and $|\phi_k\rangle = \prod_{n=1}^k [V_n(\boldsymbol{\theta}_n) W_n] |0\rangle$. From the product rule, the K -copy derivative of $\langle O \rangle$ is given by

$$\partial_k \langle O^{(K)} \rangle = K \langle \phi_k |^{\otimes K} U_k^{\dagger \otimes K} O^{(K)} U_k^{\otimes K} \left[\left(-i\frac{1}{2}\sigma_k\right) \otimes I^{\otimes K-1} \right] |\phi_k\rangle^{\otimes K} + \text{h.c.}\tag{S6}$$

In the above, the states are freely rearranged while the factor of K emerges from the product rule. We now define $O' = U_k^{\dagger \otimes K} O^{(K)} U_k^{\otimes K}$. Then, applying Eq. (S6) in the second row gives

$$\begin{aligned}\partial_k \langle O \rangle &= \frac{K}{4} \langle \phi_k |^{\otimes K} O' [(-i\sigma_k) \otimes I^{\otimes K-1}] |\phi_k\rangle^{\otimes K} + \text{h.c.} \\ &= \frac{K}{4} [\langle \phi_k |^{\otimes K} [(I - i\sigma_k)^\dagger \otimes I^{\otimes K-1}] O' [(I - i\sigma_k) \otimes I^{\otimes K-1}] |\phi_k\rangle^{\otimes N} \\ &\quad - \langle \phi_k |^{\otimes K} [(I + i\sigma_k)^\dagger \otimes I^{\otimes K-1}] O' [(I + i\sigma_k) \otimes I^{\otimes K-1}] |\phi_k\rangle^{\otimes K}].\end{aligned}\tag{S7}$$

For any Pauli strings σ_k , we can use Eq. (S5) to find

$$\begin{aligned}\partial_k \langle O \rangle &= \frac{K}{2} \left[\langle \phi_k |^{\otimes K} \left[e^{-i\frac{\pi}{2}\frac{1}{2}\sigma_k} \otimes I^{\otimes K-1} \right]^\dagger O' \left[e^{-i\frac{\pi}{2}\frac{1}{2}\sigma_k} \otimes I^{\otimes K-1} \right] |\phi_k\rangle^{\otimes K} \right. \\ &\quad \left. - \langle \phi_k |^{\otimes K} \left[e^{i\frac{\pi}{2}\frac{1}{2}\sigma_k} \otimes I^{\otimes K-1} \right]^\dagger O' \left[e^{i\frac{\pi}{2}\frac{1}{2}\sigma_k} \otimes I^{\otimes K-1} \right] |\phi_k\rangle^{\otimes K} \right] \\ &= \frac{K}{2} \left[\langle \psi(\boldsymbol{\theta} + \frac{\pi}{2}\mathbf{e}_k) | \langle \psi(\boldsymbol{\theta}) |^{\otimes K-1} O^{(K)} | \psi(\boldsymbol{\theta} + \frac{\pi}{2}\mathbf{e}_k) \rangle | \psi(\boldsymbol{\theta}) \rangle^{\otimes K-1} \right. \\ &\quad \left. - \langle \psi(\boldsymbol{\theta} - \frac{\pi}{2}\mathbf{e}_k) | \langle \psi(\boldsymbol{\theta}) |^{\otimes K-1} O^{(K)} | \psi(\boldsymbol{\theta} - \frac{\pi}{2}\mathbf{e}_k) \rangle | \psi(\boldsymbol{\theta}) \rangle^{\otimes K-1} \right],\end{aligned}\tag{S8}$$

where we have introduced the k th unit vector \mathbf{e}_k and absorbed the exponential into the definition of the k th parameterized rotation: $U_k e^{-i\frac{\pi}{2}\frac{1}{2}\sigma_k} |\phi_k\rangle = |\psi(\boldsymbol{\theta} + \frac{\pi}{2}\mathbf{e}_k)\rangle$. We can now get the n -th moment of the Pauli spectrum simply by setting $K = 2n$ and performing Bell measurements.

To compute the gradient of the Tsallis SE in respect to the k th parameter, we have

$$\partial_k T_n = (1 - n)^{-1} \partial_k A_n,\tag{S9}$$

where $A_n = \langle \psi |^{\otimes 2n} \Gamma_n^{\otimes N} | \psi \rangle^{\otimes 2n}$. For the Rényi SE, we have

$$\partial_k M_n = (1 - n)^{-1} \frac{1}{A_n} \partial_k A_n.\tag{S10}$$

Now, we present the algorithm to efficiently compute an unbiased estimator of the gradient of the SE on quantum computers for odd $n > 1$. The algorithm is detailed in Algorithm 3. The algorithm computes the gradient of A_n using the shift-rule. To calculate the gradient, one performs Bell measurements on a parameterized quantum state shifted by $\pm\pi/2$ with $|\psi(\boldsymbol{\theta} \pm \pi/2)\rangle | \psi(\boldsymbol{\theta})\rangle$, as well as $n - 1$ Bell measurements on states without shift $|\psi(\boldsymbol{\theta})\rangle | \psi(\boldsymbol{\theta})\rangle$. Then, use the same procedure as Algorithm 1 in the main text to estimate K_\pm , where its difference scaled by n gives us $\partial_k A_n$.

Supplemental Materials D: Strong monotonicity and measuring Rényi SEs

A not necessary, but useful property of nonstabilizerness is strong monotonicity where the measure is on average non-increasing under computational-basis measurements on a set of k qubits [47]. This property demands that $T_n(|\psi\rangle) \geq \sum_\lambda p_\lambda T_n[|\psi_\lambda\rangle]$ when using the projector $\Pi_\lambda = |\lambda\rangle\langle\lambda| \otimes \mathbf{1}_{N\setminus k}$ onto the computational basis state λ with

Algorithm 3: Gradient of SE

Input : Integer $n > 1$
 L repetitions
 Circuit parameter θ
 N -qubit parameterized unitary $U(\theta)$
 Gradient parameter index k

Output: Gradient $\partial_k A_n$

```

1 for  $s = -1, +1$  do
2    $B_s = 0$ 
3   for  $q = 1, \dots, L$  do
4     Prepare  $|\eta_{\text{shifted}}\rangle = U_{\text{Bell}}^{\otimes N}(U(\theta + s e_k) \otimes U(\theta)) |0\rangle^{\otimes 2N}$ 
5     Sample in computational basis  $\mathbf{r}^{(1)} \sim |\langle \mathbf{r} | \eta_{\text{shifted}} \rangle|^2$ 
6     for  $j = 1, \dots, n-1$  do
7       Prepare  $|\eta\rangle = U_{\text{Bell}}^{\otimes N}(U(\theta) \otimes U(\theta)) |0\rangle^{\otimes 2N}$ 
8       Sample in computational basis  $\mathbf{r}^{(j+1)} \sim |\langle \mathbf{r} | \eta \rangle|^2$ 
9     end
10     $b = 1$ 
11    for  $\ell = 1, \dots, N$  do
12       $\nu_1 = \bigoplus_{j=1}^n r_{2^{\ell-1}}^{(j)}$ 
13       $\nu_2 = \bigoplus_{j=1}^n r_{2^\ell}^{(j)}$ 
14      if  $n$  is odd then
15         $b = b \cdot (-2\nu_1 \cdot \nu_2 + 1)$ 
16      else
17         $b = b \cdot 2(\nu_1 - 1) \cdot (\nu_2 - 1)$ 
18      end
19    end
20     $B_s = B_s + b/L$ 
21  end
22 end
23  $\partial_k A_n = n(B_+ - B_-)$ 

```

corresponding probability $p_\lambda = \langle \psi | \Pi_\lambda | \psi \rangle$ and post-measurement state $|\psi_\lambda\rangle$. The Rényi SE M_n is not a strong monotone for all n [17]. For $n < 2$, we can show that the Tsallis SE T_n is not a strong monotone. However, for $n \geq 2$ we are unable to find any example where strong monotonicity is violated. Using extensive numerical optimization for the strong monotonicity condition, we find strong evidence that T_n for $n \geq 2$ is a strong monotone for at least $N \leq 6$ qubits.

We now discuss the scaling of measuring the Rényi SE. We can estimate $A_n = 2^{-N} \sum_{\sigma \in \mathcal{P}} \langle \psi | \sigma | \psi \rangle^{2n}$ with additive precision using $O(n\epsilon^{-2})$ samples with our algorithms. The Rényi SE involves the logarithm of A_n , i.e. $M_n \sim \ln(A_n)$. Given A_n estimated with additive precision ϵ , we now consider the cost of estimating M_n with additive precision ϵ_M . Given exact \bar{A}_n and \bar{M}_n , we assume from finite samples we have error ϵ in estimating A_n , which gives us

$$(1-n)^{-1} \ln(\bar{A}_n - \epsilon) = \bar{M}_n + \epsilon_M. \quad (\text{S1})$$

We insert $A_n = \exp(M_n(1-n))$ to get

$$\epsilon_M = (1-n)^{-1} \ln(1 - e^{-\bar{M}_n(1-n)} \epsilon) \quad (\text{S2})$$

We now assume $\epsilon \ll \bar{A}_n$ and get

$$\epsilon_M \approx -(1-n)^{-1} e^{-\bar{M}_n(1-n)} \epsilon \quad (\text{S3})$$

and finally

$$\epsilon \approx -(1-n) e^{\bar{M}_n(1-n)} \epsilon_M. \quad (\text{S4})$$

For $n > 1$, to estimate M_n with precision ϵ_M , we require an accuracy $\epsilon = O(\exp(-M_n)\epsilon_M)$ exponentially small in M_n . With our algorithm this requires a number of samples $O(\exp(M_n)\epsilon_M^{-2})$ scaling in general exponentially in M_n . Assuming $M_n = \log(n)$, one can estimate M_n with polynomial number of measurements.

Note that this challenge in estimating the logarithm of a function appears for any entropy involving logarithms, such as for the 2-Rényi entanglement entropy $\text{tr}(\rho^2)$ and $-\log(\text{tr}(\rho^2))$.

Supplemental Materials E: Other nonstabilizerness monotones and known bounds

We introduce different magic monotones, and reproduce the proof of upper bound of stabilizer fidelity. First, the robustness of magic for state ρ is given by [8]

$$R(\rho) = \min_x \left(\sum_k |x_k|; \rho = \sum_k x_k |\phi_k\rangle \langle \phi_k| \right), \quad (\text{S1})$$

where $x_k \in \mathbb{R}$ and $|\phi_k\rangle \in \text{STAB}$ are stabilizer states. The stabilizer extent for a pure state $|\psi\rangle$ is given by [49]

$$\xi(|\psi\rangle) = \min_c \left(\sum_k |c_k|; |\psi\rangle = \sum_k c_k |\phi_k\rangle \right)^2, \quad (\text{S2})$$

where $c_k \in \mathbb{C}$. Finally, the stabilizer fidelity measures the geometric distance to the closest stabilizer state [49]

$$F_{\text{STAB}}(|\psi\rangle) = \max_{|\phi\rangle \in \text{STAB}} |\langle \psi | \phi \rangle|^2. \quad (\text{S3})$$

The moment of the Pauli spectrum A_n for $n > 1$ upper bounds the stabilizer fidelity, which was previously proven in Ref. [17] via the Rényi SE. Here, we reproduce the proof for completeness and adapt it to our efficient measurement algorithms. First, we note that for any state $|\psi\rangle$ with stabilizer fidelity $F_{\text{STAB}}(|\psi\rangle)$ one can find a Clifford unitary U_C with

$$|\phi\rangle = U_C |\psi\rangle = \sum_k a_k |k\rangle, \quad (\text{S4})$$

where

$$|a_0|^2 = F_{\text{STAB}}(|\psi\rangle). \quad (\text{S5})$$

One can see this immediately from $F_{\text{STAB}} = |\langle \psi | \phi_{\text{max}} \rangle|^2 = |\langle \psi | U_C^{\text{max}} | 0 \rangle|^2 = |a_0|^2$. In Eq. (S4), we denote $\{|k\rangle\}$ the computational basis states. Next, we have

$$2^{-N} \sum_{\sigma \in \mathcal{P}} |\langle \phi | \sigma | \phi \rangle|^{2n} \geq 2^{-N} \sum_{\sigma \in \mathcal{P}_z} |\langle \phi | \sigma | \phi \rangle|^{2n} \geq 2^{-2nN} \left(\sum_{\sigma \in \mathcal{P}_z} |\langle \phi | \sigma | \phi \rangle| \right)^{2n}. \quad (\text{S6})$$

Here \mathcal{P} is the set of all Pauli strings while \mathcal{P}_z is the set of Pauli strings which contains strings with $\mathbb{1}$ and σ^z only. We have used the convexity inequality

$$\sum_{i=1}^m |a_i|^k \geq \frac{1}{m^{k-1}} \left(\sum_{i=1}^m |a_i| \right)^k. \quad (\text{S7})$$

Now, we apply

$$\left(\sum_{\sigma \in \mathcal{P}_z} |\langle \phi | \sigma | \phi \rangle| \right)^{2n} \geq \left| \sum_{\sigma \in \mathcal{P}_z} \langle \phi | \sigma | \phi \rangle \right|^{2n}, \quad (\text{S8})$$

and the fact that

$$\sum_{\sigma \in \mathcal{P}_z} \sigma = 2^N |0\rangle \langle 0|, \quad (\text{S9})$$

together with Eq. (S6) to get

$$2^{-N} \sum_{\sigma \in \mathcal{P}} |\langle \phi | \sigma | \phi \rangle|^{2n} \geq |a_0|^{4n} = F_{\text{STAB}}(|\psi\rangle)^{2n}. \quad (\text{S10})$$

Then, we use the fact that A_n is invariant under unitary operations to get $\sum_{\sigma \in \mathcal{P}} |\langle \phi | \sigma | \phi \rangle|^{2n} = \sum_{\sigma \in \mathcal{P}} |\langle \psi | \sigma | \psi \rangle|^{2n}$. We insert the definition of T_n to finally get

$$F_{\text{STAB}}(|\psi\rangle) \leq A_n(|\psi\rangle)^{\frac{1}{2n}}, \quad (\text{S11})$$

which concludes the proof of the upper bound. Furthermore, we note the well known relationship between R , ξ and F_{STAB} [12, 49]

$$R \geq \xi \geq F_{\text{STAB}}^{-1}, \quad (\text{S12})$$

which combined gives us the final bound:

$$R \geq \xi \geq F_{\text{STAB}}^{-1} \geq A_n^{-\frac{1}{2n}}. \quad (\text{S13})$$

Supplemental Materials F: Proof of lower bound of stabilizer fidelity

Here, we prove that the n th moment of the Pauli spectrum A_n is a lower bound of the stabilizer fidelity F_{STAB} . The main ingredient is the relationship proven in [39, 51]

$$F_{\text{STAB}}(|\psi\rangle) \geq 2^{-N} \sum_{\sigma \in \mathcal{Q}} \langle \psi | \sigma | \psi \rangle^2, \quad (\text{S1})$$

where $\mathcal{Q} = \{\sigma \in \mathcal{P} : \langle \psi | \sigma | \psi \rangle^2 > \frac{1}{2}\}$. We now have

$$\begin{aligned} F_{\text{STAB}} &\geq 2^{-N} \sum_{\sigma \in \mathcal{Q}} \langle \psi | \sigma | \psi \rangle^2 = \Pr_{\sigma \sim \Xi(\sigma)} [\langle \psi | \sigma | \psi \rangle^2 > \frac{1}{2}] = \Pr_{\sigma \sim \Xi(\sigma)} [\langle \psi | \sigma | \psi \rangle^{2(n-1)} > 2^{1-n}] \\ &= 1 - \Pr_{\sigma \sim \Xi(\sigma)} [\langle \psi | \sigma | \psi \rangle^{2(n-1)} \leq 2^{1-n}] = 1 - \Pr_{\sigma \sim \Xi(\sigma)} [1 - \langle \psi | \sigma | \psi \rangle^{2(n-1)} \geq 1 - 2^{1-n}] \\ &\geq 1 - \frac{1}{1 - 2^{1-n}} (1 - \mathbb{E}_{\sigma \sim \Xi(\sigma)} [\langle \psi | \sigma | \psi \rangle^{2(n-1)}]) = 1 - \frac{1}{1 - 2^{1-n}} (1 - \sum_{\sigma \in \mathcal{P}} \frac{\langle \psi | \sigma | \psi \rangle^{2n}}{2^N}) \\ &= \frac{A_n - 2^{1-n}}{1 - 2^{1-n}}. \end{aligned} \quad (\text{S2})$$

In the first line we used the definition of \mathcal{Q} , and in the second line we used Markov's inequality which holds for $n > 1$.

Supplemental Materials G: Relationship of measures of nonstabilizerness

Here we study the relationship of different measures of nonstabilizerness. In particular, we study the Rényi SE M_n , the min-relative entropy of magic $D_{\text{min}} = -\ln(F_{\text{STAB}})$, the log-free robustness of magic LR = $\ln(R)$ and the max-relative entropy of magic $\ln(\xi)$. We also consider the additive Bell magic [14] which is defined and further discussed in SM K.

We now study the N -qubit product state

$$|\psi(s)\rangle = 2^{-N/2} (|0\rangle + \exp(i\pi s/4) |1\rangle)^{\otimes N}. \quad (\text{S1})$$

We study the scaling of this state with s . We show the scaling in Fig. S1.

For D_{min} , \mathcal{B}_a and M_n with $n \geq 2$ we find that these measures of nonstabilizerness scale as $\propto s^2 N$. Defining $\theta = s\sqrt{N}$, we find for all these measures $\propto \theta^2$. This indicates that these measure are closely related. We study the relationship between these measures further by finding respective upper and lower bounds. We numerical maximize and minimize the ratios D_{min}/M_n and \mathcal{B}_a/M_n over all pure states for a given qubit number N . This gives us a lower and upper bound between these measures. Due to numerical complexity of computing D_{min} and \mathcal{B}_a exactly, we can optimize up to $N \leq 4$. We find that the bounds barely change with N , indicating that they are likely valid even for higher qubit numbers. In particular, we find $1.7M_2 \gtrsim D_{\text{min}} \geq \frac{1}{4}M_2$ as well as $3.5M_2 \gtrsim \mathcal{B}_a \gtrsim 2.88M_2$ for at least $N \leq 4$.

In contrast, for LR, D_{max} and $M_{1/2}$ we find that these measures scale as $\propto sN$ and thus $\propto \theta/\sqrt{N}$. These measures show a different scaling with N compared to the measures that relate to geometric distance such as D_{min} . This shows that LR, D_{max} and $M_{1/2}$ do not support upper bounds in respect to M_n for $n > 1/2$. As there are no known efficient measurement protocols for $M_{1/2}$, it is likely that one cannot find efficiently measurable upper bounds for D_{max} and LR.

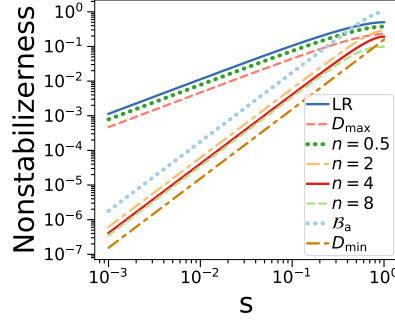


Figure S1. Scaling of different measures of nonstabilizerness for state Eq. (S1) as function of s .

Supplemental Materials H: Error mitigation

Noise in the quantum computer distorts the true value of the SE. We now propose how to mitigate noise without requiring additional measurements. Here, we assume that a pure state $|\psi\rangle$ is subject to a global depolarizing channel with probability p , resulting in the noisy state $\rho_{\text{dp}} = (1-p)|\psi\rangle\langle\psi| + pI_N 2^{-N}$. The depolarising probability p can be deduced by the measurement of purity $\text{tr}(\rho_{\text{dp}}^2)$ as shown in Ref. [14]

$$p = 1 - \frac{\sqrt{(2^N - 1)(2^N \text{tr}(\rho_{\text{dp}}^2) - 1)}}{2^N - 1}. \quad (\text{S1})$$

Note that $\text{tr}(\rho_{\text{dp}}^2)$ can be efficiently measured with Bell measurements [62]. In particular, the purity can be measured via $\text{tr}(\rho_{\text{dp}}^2) = A_1$ using Algorithm 1 in an efficient manner. SEs for depolarized state ρ_{dp} can be expressed using the expectation value of operator $\Gamma_n^{\otimes N} = 2^{-N} \sum_{\sigma \in \mathcal{P}} \sigma^{\otimes 2n}$ acting on $2n$ copies of the mixed state ρ_{dp}

$$\begin{aligned} A_n^{\text{dp}} &= \text{tr}(\rho_{\text{dp}}^{\otimes 2n} \Gamma_n^{\otimes N}) = \frac{1}{2^N} \sum_{\sigma \in \mathcal{P}} [\text{tr}(\rho_{\text{dp}} \sigma)]^{2n} = \frac{1}{2^N} \sum_{\sigma \in \mathcal{P}} [(1-p)\langle\psi|\sigma|\psi\rangle + p\delta_{\sigma, I_N}]^{2n} \\ &= \frac{(1-p)^{2n}}{2^N} \sum_{\sigma \in \mathcal{P}} \langle\psi|\sigma|\psi\rangle^{2n} + \frac{1 - (1-p)^{2n}}{2^N} = (1-p)^{2n} A_n^{\text{mtg}} + \frac{1 - (1-p)^{2n}}{2^N}, \end{aligned} \quad (\text{S2})$$

where A_n^{mtg} is the mitigated expectation value using the measurement result affected by depolarizing noise A_n^{dp} . We find

$$A_n^{\text{mtg}} = \frac{A_n^{\text{dp}}}{(1-p)^{2n}} - \frac{(1-p)^{-2n} - 1}{2^N}. \quad (\text{S3})$$

We then substitute the above expression to calculate $T_n = -(1 - A_n)/(1 - n)$, to realize the expression of mitigated SE T_n^{mtg} in terms of depolarized SE T_n^{dp}

$$T_n^{\text{mtg}} = \frac{1}{(1-p)^{2n}} \left[T_n^{\text{dp}} - \frac{(1 - (1-p)^{2n})(2^{-N} - 1)}{(1-n)} \right]. \quad (\text{S4})$$

Similarly, we have for the Rényi SE

$$M_n^{\text{mtg}} = (1-n)^{-1} \ln(A_n^{\text{mtg}}). \quad (\text{S5})$$

Supplemental Materials I: Further IonQ quantum computer results

In Fig. S2 we demonstrate our lower bounds for robustness of magic R and stabilizer extent ξ using our Algorithm 1 for the Pauli spectrum moments $A_n = 2^{-N} \sum_{\sigma \in \mathcal{P}} \langle\psi|\sigma|\psi\rangle^{2n}$. We compute the bounds using the error mitigated measured A_2 and A_3 using Algorithm 1 of the main text. We show the upper bound $F_{\text{STAB}} \leq A_n^{\frac{1}{2n}}$ and the lower

bounds $\xi \geq A_n^{-\frac{1}{2n}}$. Further, we show $R \geq A_n^{\frac{1}{2(1-n)}}$ which is the improved bound only valid for R . For A_2 , Algorithm 1 is not efficient, however for our chosen qubit number and measurement samples we are able to achieve sufficient accuracy.

We find that the exactly simulated bounds closely match the result from the IonQ quantum computer. We find the bounds for A_2 and A_3 show similar result, except for R where we find that A_2 gives a better bound.

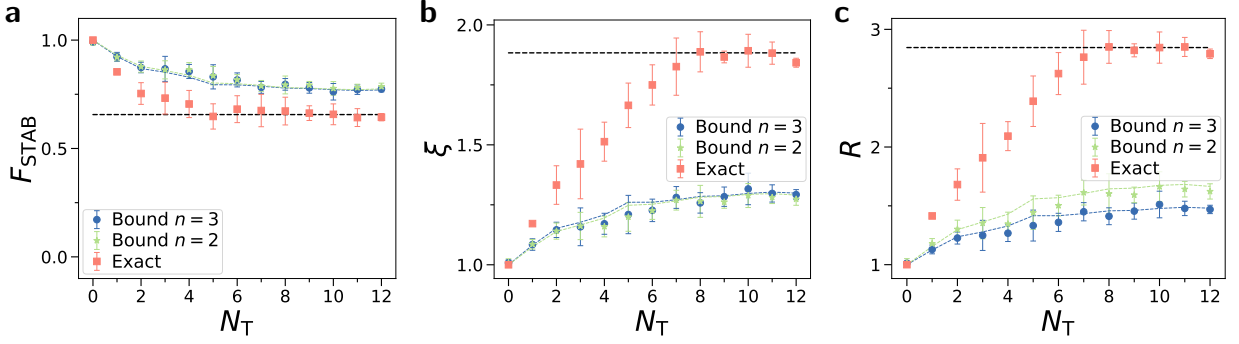


Figure S2. Compute bounds for other nonstabilizerness monotones by using A_2 and A_3 . **a)** Stabilizer fidelity F_{STAB} , **b)** Stabilizer extent ξ and **c)** robustness of magic R . Orange dots indicate exact simulation of the measure. Blue and green dots are bounds from error mitigated measurements, while dashed lines indicate bounds computed using the simulated A_n . We show quantum states generated by random Clifford circuits doped with N_T T-gates on the IonQ quantum computer, where we compute 6 random instances of the state. We have $N = 3$ qubits, $L = 10^3$ Bell measurements and a measured depolarization error of $p \approx 0.1$.

Finally, we also demonstrate measurement of the Tsallis entropy T_5 in Fig. S3. We find similar behavior to T_3 as measured in the main text.

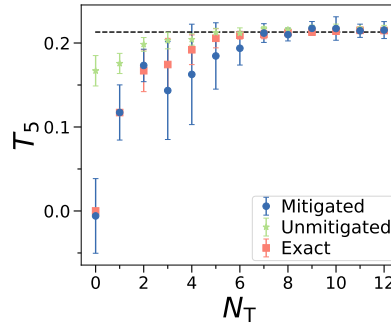


Figure S3. Measurement of T_5 with and without error mitigation. Dashed line is average value of T_5 for Haar random states.

Supplemental Materials J: Error mitigation for different noise models

We now study the performance of our error mitigation strategy for different noise models. Our error mitigation strategy assumes global depolarization noise, which is a simple noise model. Our experiment indicate that it works well even for the noise of the IonQ quantum computer which is known to have a more complex noise model. Here, we provide further simulations with various noise models, finding that our model performs surprisingly well, both for unital and non-unital noise models.

We simulate random Clifford circuits constructed from layers of single-qubit rotations and CNOT gates arranged in a nearest-neighbor configuration, where we can dope the circuit with N_T T-gates. After every gate, we apply a noise channel with noise strength p on the qubits the gate acted on.

We study the following three noise models, which have the following channel description for each qubit: For unital noise, we consider local depolarizing noise

$$\Lambda_{\text{Idp}}(\rho) = (1 - p)\rho + p/2I_1, \quad (\text{S1})$$

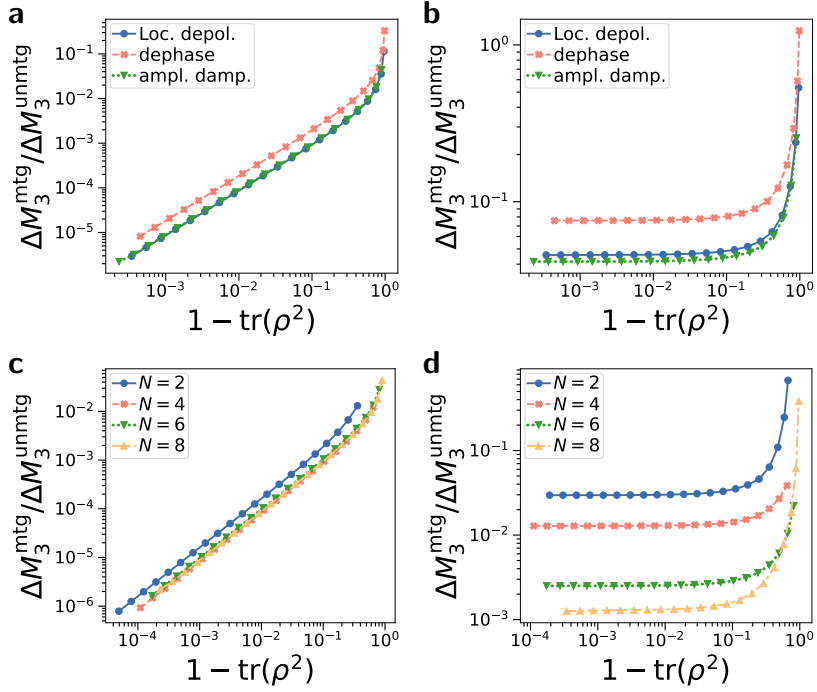


Figure S4. We simulate our error mitigation strategy for local depolarizing, dephasing and amplitude dampening noise. The noise channel is applied after each gate, where we consider layered single qubit and CNOT gates forming random Clifford circuits. We show relative error $\Delta M_\alpha^{\text{mtg}} / \Delta M_\alpha^{\text{unmtg}}$ against impurity $1 - \text{tr}(\rho^2)$. Each point is averaged over 20 random instances. **a,c)** We show random Clifford circuits, while in **b,d)** we show Clifford circuits doped with $N_T = N$ T-gates. We show **a,b)** different noise models for $N = 8$ qubits, while in **c,d)** we show different number of qubits N for amplitude dampening noise.

local dephasing noise

$$\Lambda_{\text{dephase}}(\rho) = (1 - p)\rho + p\sigma^z\rho\sigma^z. \quad (\text{S2})$$

Further, we consider the amplitude dampening channel as a non-unital noise channel

$$\Lambda_a(\rho) = (1 - p)\rho + p\sigma^- \rho \sigma^+. \quad (\text{S3})$$

To quantify the performance of the error mitigation, we compute the error in SE without error mitigation

$$\Delta M_\alpha^{\text{unmtg}} = |M_\alpha^{\text{unmtg}} - M_\alpha^{\text{pure}}| \quad (\text{S4})$$

and with error mitigation

$$\Delta M_\alpha^{\text{mtg}} = |M_\alpha^{\text{mtg}} - M_\alpha^{\text{pure}}| \quad (\text{S5})$$

where M_α^{pure} is the noise-free SE, M_α^{unmtg} the unmitigated SE and M_α^{mtg} the mitigated SE. We consider now the ratio $\Delta M_\alpha^{\text{mtg}} / \Delta M_\alpha^{\text{unmtg}}$, which indicates the relative error reduction with error mitigation, which is smaller 1 when error mitigation yields an improvement.

We show the relative error for different noise models against impurity $1 - \text{tr}(\rho^2)$ in Fig. S4. We show simulation results for random Clifford circuits in Fig. S4a,c and Clifford circuits doped with $N_T = N$ T-gates in Fig. S4b,d. In Fig. S4a,b we find that error mitigation provides a substantial improvement in error for all considered noise models, both for unital and non-unital noise. For Clifford circuits, we find empirically a linear relationship $\Delta M_\alpha^{\text{mtg}} / \Delta M_\alpha^{\text{unmtg}} \propto 1 - \text{tr}(\rho^2)$ between relative error and impurity. Whereas for doped Clifford circuits the improvement converges to a constant for small $1 - \text{tr}(\rho^2)$.

In Fig. S4c,d, we show amplitude dampening noise for different number of qubits N . We find that the reduction in error due to error mitigation is independent of qubit number for Clifford circuits, while for doped Clifford circuits the error decreases even further with N . This indicates that our error mitigation strategy can work well even for more qubits.

Supplemental Materials K: Bell measurements, stabilizer entropy and Bell magic

Bell measurements are a powerful measurement scheme to estimate non-linear properties of quantum states. One takes two copies $|\psi\rangle|\psi\rangle$ and transforms them into the Bell basis via U_{Bell} as described in the main text. Sampling in the Bell basis gives an $2N$ bit outcome \mathbf{r} with a probability [40]

$$P(\mathbf{r}) = 2^{-N} |\langle\psi|\sigma_{\mathbf{r}}|\psi^*\rangle|^2, \quad (\text{S1})$$

where $\sigma_{\mathbf{r}}$ is a Pauli string. Bell measurements can be used to measure the purity, fidelity (as they realize a destructive SWAP test [62]), entanglement [62], coherence, imaginarity [44] and estimate the absolute values of any Pauli expectation value as a type of shadow tomography [54]. Further, Bell measurements can be used to learn stabilizer states [40]. All these properties can be extracted at the same time by using different post-processing steps.

For example to measure purity $\text{tr}(\rho^2)$, one performs a logical AND on outcome \mathbf{r} between each qubit pair corresponding to the first and second copy, then compute its parity [62].

For learning stabilizers, the core routine is Bell difference sampling [39]. Here, one performs two Bell measurements with outcomes \mathbf{r}, \mathbf{r}' and takes their difference $\mathbf{q} = \mathbf{r} - \mathbf{r}'$.

The probability of outcome \mathbf{q} for Bell difference sampling is given by [39]

$$\begin{aligned} Q(\mathbf{q}) &= \sum_{\mathbf{r} \in \{0,1\}^{2N}} P(\mathbf{r})P(\mathbf{r} \oplus \mathbf{q}) = 4^{-N} \sum_{\mathbf{r} \in \{0,1\}^{2N}} |\langle\psi|\sigma_{\mathbf{r}}|\psi^*\rangle|^2 |\langle\psi|\sigma_{\mathbf{r} \oplus \mathbf{q}}|\psi^*\rangle|^2 \\ &= 4^{-N} \sum_{\mathbf{r} \in \{0,1\}^{2N}} |\langle\psi|\sigma_{\mathbf{r}}|\psi\rangle|^2 |\langle\psi|\sigma_{\mathbf{r} \oplus \mathbf{q}}|\psi\rangle|^2 = 4^{-N} \sum_{\mathbf{r} \in \{0,1\}^{2N}} |\langle\psi|\sigma_{\mathbf{r}}|\psi\rangle|^2 |\langle\psi|\sigma_{\mathbf{r}}\sigma_{\mathbf{q}}|\psi\rangle|^2. \end{aligned}$$

The last step follows from the commutation rules of Pauli operators which gives $|\langle\psi|\sigma_{\mathbf{r} \oplus \mathbf{q}}|\psi\rangle| = |\langle\psi|\sigma_{\mathbf{r}}\sigma_{\mathbf{q}}|\psi\rangle|$, while the derivation for the second last step can be found in [14, 39].

When $|\psi\rangle$ is a stabilizer state, then it is described by a commuting group of Pauli G with expectation value $|\langle\psi|\sigma|\psi\rangle|^2 = 1, \forall \sigma \in G$. In the commuting group $\sigma, \sigma' \in G$, the commutator is zero with $[\sigma, \sigma'] = 0$. For all other Pauli strings $\sigma \notin G$ we have $|\langle\psi|\sigma|\psi\rangle|^2 = 0$. Thus, only when $|\psi\rangle$ is a stabilizer state, one can show that $Q(\mathbf{q}) = 2^{-N} |\langle\psi|\sigma_{\mathbf{q}}|\psi\rangle|^2$. Or in other words, for stabilizer states, Bell difference sampling samples Pauli strings $\sigma_{\mathbf{q}}$ according to the Pauli spectrum $\Xi(\sigma_{\mathbf{q}}) = 2^{-N} |\langle\psi|\sigma_{\mathbf{q}}|\psi\rangle|^2$ and all sampled Pauli strings must commute.

This commuting property is used in Bell magic \mathcal{B} to generate a measure of nonstabilizerness [14]

$$\mathcal{B}(|\psi\rangle) = \sum_{\mathbf{r}, \mathbf{q} \in \{0,1\}^{2N}} Q(\mathbf{r})Q(\mathbf{q}) \|\sigma_{\mathbf{r}}, \sigma_{\mathbf{q}}\|_{\infty} \quad (\text{S2})$$

where the infinity norm is zero $\|\sigma_{\mathbf{r}}, \sigma_{\mathbf{q}}\|_{\infty} = 0$ when the two Pauli strings commute $[\sigma_{\mathbf{r}}, \sigma_{\mathbf{q}}] = 0$, and $\|\sigma_{\mathbf{r}}, \sigma_{\mathbf{q}}\|_{\infty} = 2$ otherwise. Correspondingly, the additive Bell magic is defined as $\mathcal{B}_a = -\log_2(1 - \mathcal{B})$. Due to the commuting property, only for pure stabilizer states $|\psi_{\text{C}}\rangle$ we have $\mathcal{B}(|\psi_{\text{C}}\rangle) = 0$, else it is greater zero. One can also check that it is invariant under Clifford unitaries. We also note that the complexity of the error mitigation scheme for Bell magic scales as $1/(1-p)^8$ where p is the depolarization probability. In contrast, for stabilizer entropy it scales as $1/(1-p)^{2n}$, e.g. for $n = 3$ we have $1/(1-p)^6$.

The measurement protocols for stabilizer entropy uses a different method to measure nonstabilizerness. In particular, one has to measure the operator $\Gamma^{\otimes N} = \sum_{\sigma \in \mathcal{P}} \sigma^{\otimes 2n}$ which measures the n -th moment of the Pauli spectrum. This operator is diagonalized by Bell transformations as shown in SM B. By appropriately post-processing of Algorithm 1 in the main text one can then measure

$$A_n = 2^{-N} \sum_{\sigma \in \mathcal{P}} \langle\psi|\sigma|\psi\rangle^{2n} = \langle\psi|^{\otimes 2n} \Gamma_n^{\otimes N} |\psi\rangle^{\otimes 2n}. \quad (\text{S3})$$

Note that the fact that Pauli strings of stabilizer states commute is not used at all, in contrast to Bell magic. Instead, stabilizer entropy is a measure of the moment of the Pauli spectrum determine nonstabilizerness. In particular, stabilizer states have a peaked Pauli distribution with either $|\langle\psi|\sigma|\psi\rangle|^2 = 0$ or $|\langle\psi|\sigma|\psi\rangle|^2 = 1$. In contrast, highly magical states have a broad distribution $|\langle\psi|\sigma|\psi\rangle|^2 \approx 4^{-N}$.

Our Algorithm 2 uses yet another approach to measure the stabilizer entropy. It samples directly from the Pauli spectrum (via the complex conjugate $|\psi^*\rangle$) in a Monte-Carlo fashion and then averages over the sampled Pauli strings via

$$A_n = \mathbb{E}_{\sigma \sim \Xi(\sigma)} [\langle\psi|\sigma|\psi\rangle^{2n-2}]. \quad (\text{S4})$$